Fidelity of photon propagation in electromagnetically induced transparency in the presence of four-wave mixing

Nikolai Lauk,[1,*] Christopher O'Brien,[1] and Michael Fleischhauer[1]

[1]*Department of Physics and research center OPTIMAS University of Kaiserslautern, D-67663 Kaiserslautern, Germany*

(Dated: April 9, 2013)

We study the effects of the four-wave mixing (4WM) in a quantum memory scheme based on electromagnetically induced transparency (EIT). We treat the problem of field propagation on the quantum mechanical level, which allows us to calculate the fidelity for propagation for a quantum light pulse such as a single photon. While 4WM can be beneficial for classical, all-optical information storage, the quantum noise associated with the signal amplification and idler generation is in general detrimental for a quantum memory. We identify a range of parameters where 4WM makes a single photon quantum memory impossible.

PACS numbers: 42.50.Gy, 42.50.Ct, 03.67.Hk, 42.65-k

I. INTRODUCTION

A reliable quantum memory for photons is one of the essential ingredients for quantum networks and optical quantum computing. There have been several proposals for photon storage, which fall into three main categories: gradient echo techniques [1], far detuned Raman systems [2], and electromagnetically induced transparency (EIT) [3]. In all these schemes the storage of single photons occurs by mapping the quantum state of photons onto a long lived atomic excitation.

In this paper we will concentrate on the EIT based scheme, where one uses a strong control field to couple an incoming signal pulse to the atomic spin coherence resulting in the common propagation of both as a dark state polariton. By adiabatically switching off the control field the signal field is mapped on the spin coherence and later, after some storage time, is retrieved by switching on the control field. Since its theoretical proposal [4, 5] and the first experimental realizations[6, 7] there has been a large development of EIT based quantum memories (QM), e.g. successful implementation in hot gases [8], in cold gases using magneto-optical traps (MOT) [9] or optical lattices [10, 11], as well as solid systems such as rare-earth doped crystals [12]. E.g., using EIT memory in gases, weak coherent pulses have been stored in hot Rubidium gas with storage times of $T_s = 1ms$ and storage efficiencies of $\eta_m = 45\%$ [13]. While in a cold Rb MOT, EIT has been used to store pulses with storage times of $T_s = 1ms$, with $\eta_m = 78\%$ [14].

The storage efficiency of EIT QM is limited by two considerations. First the spatial pulse size L_p must fit entirely inside of the medium $L_p = T_p v_g < L$, where T_p is the pulse duration and v_g is the group velocity in the medium, otherwise some of the pulse will leak out during the storage process and be lost. Secondly, the spectral width of the pulse $\Delta\omega_p$ must be well within the EIT transmission window, $\Delta\omega_p \ll \omega_{EIT} \simeq \sqrt{D} v_g/L$, where $D = L/L_{\rm abs}$ denotes the optical depth of the medium, i.e. the ratio of medium length L to absorption length $L_{\rm abs}$ in the absence of EIT. Since the spectral width and pulse length are inversely proportional $\Delta\omega_p \sim 1/T_p$, these two requirements compete with each other and both of them can only be satisfied at large optical depth $\sqrt{D} \gg 1$ [15].

However with high optical depth, non-linear processes start to become important. In particular, a four wave mixing process (4WM) is possible in many of the implementations of EIT QM, where the control field with Rabi frequency Ω and appropriate polarization also acts as a far-detuned field with Rabi frequency Ω' on the signal transition spontaneously generating a new 'idler' field. This idler field then moves population into the spin state, which is then pumped by the control field to the excited state as shown in Fig. 1. The medium is still transparent to the signal pulse due to EIT, but now the signal pulse also experiences some gain from 4WM.

The role of 4WM in EIT quantum memories is not completely clear. In one experiment, 4WM was suggested as an explanation of why the storage efficiency has tended to saturate to values lower than 50% with high D in EIT QM experiments [16]. However, there have also been experiments [17] that claim 4WM may be useful due to better spatial pulse compression and pulse gain. [17] also suggests that with the help of the 4WM one may achieve multimode storage, storing not only the signal mode, but also the idler mode. However this conjecture was disproved in a more recent experiment [18] where it was clearly shown that multimode storage is not possible in this system, due to no significant slowing of an input idler field, allowing it to escape the medium before storage. Therefore, we will not consider the case of an input idler field.

EIT with 4WM has the advantage of signal gain which could be used to compensate losses in the medium, naturally improving the storage of classical signal pulses. But the goal of a quantum memory is single photon storage, where gain can become a liability since it is always accompanied by additional noise. We therefore address the case

*Electronic address: nlauk@physik.uni-kl.de

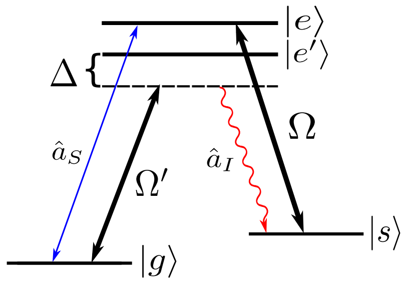

FIG. 1: Level scheme for EIT memory with four-wave mixing process. A double Λ-scheme, with one Λ being the signal field $\hat{a}_S$ and strong control field Ω giving standard EIT, and a second Λ far-detuned from resonance made up of the same control field acting on the $|g\rangle - |e'\rangle$ transition and the idler field $\hat{a}_I$ generated by 4WM.

of a single photon propagating in an EIT medium with 4WM, by developing a fully quantum model for pulse propagation in Sect. II, which we solve in Sect. III. We then analyze the amplification noise in the system in Sect. IV resulting from the spontaneous generation of idler photons coupling to the signal field. In Sect. V we use our results to calculate the memory fidelity of EIT with 4WM in an otherwise loss-less medium. In Sect. VI we consider additional linear losses and discuss the case where 4WM gain completely compensates these losses in the medium. Finally, as in EIT memories the fields are close to atomic resonances we expand our analysis in Sect. VII to incorporate noise associated with population decay from excited states.

II. MODEL

We can model the EIT 4WM system as an ensemble of four level atoms, which interact with the strong control field $\vec{E_c}$ coupling the $|s\rangle - |e\rangle$ as well as acting as a far-detuned field on the $|g\rangle - |e'\rangle$ transition and a weak co-propagating signal field $\vec{E_S}$ in resonance with the $|g\rangle - |e\rangle$ transition, see Fig. 1, a treatment similar to [19]. Due to the additional coupling of the control field to the $|g\rangle - |e'\rangle$ transition a new idler field will be generated which because of energy and momentum conservation, propagates then in the same directions as the other two fields. In this approach $|e'\rangle$ can be considered either as an additional level, or as a representation of the excited state to simplify the coupling of two fields to the same transition, in either case it will eventually be adiabatically eliminated. The interaction Hamiltonian in the dipole, rotating wave, and slowly varying envelope approximations is given by:

$$\hat{H}_{\text{int}} = \frac{\hbar N}{V}\int_0^L \mathrm{d}z \, \Big\{ \delta\hat{\sigma}_{ee} + \Delta\hat{\sigma}_{e'e'} - \left(g_S\hat{a}_S\hat{\sigma}_{eg} + g_I\hat{a}_I\hat{\sigma}_{e's} + \Omega\hat{\sigma}_{es} + \Omega'\hat{\sigma}_{e'g} + h.c. \right) \Big\} \quad (1)$$

where Δ is an effective detuning of the control laser from the $|e'\rangle - |g\rangle$ transition, δ is the detuning of the signal photon form the $|e\rangle - |g\rangle$ transition, $\Omega = \frac{\mu_{es}E_c}{\hbar}$ and $\Omega' = \frac{\mu_{e'g}E_c}{\hbar}$ are the Rabi frequencies of the control field with dipole moments μ_{eg}, $\mu_{e'g}$, N is the number of atoms in the medium, and V is the volume of the medium. $\hat{\sigma}_{\mu\nu}(z)$ are continuous atomic ensemble spin-flip operators corresponding to the transition from internal state $|\nu\rangle$ to $|\mu\rangle$, and $\hat{a}_S$ and $\hat{a}_I$ are dimensionless field operators of the signal- and idler fields, which fulfill bosonic commutation relations $[\hat{a}(z), \hat{a}^\dagger(z')] = \delta(z - z')$. $g_S = \mu_{eg}\sqrt{\frac{\omega_S}{2\hbar\epsilon_0 V}}$, $g_I = \mu_{e's}\sqrt{\frac{\omega_I}{2\hbar\epsilon_0 V}}$ are the coupling constants for the field operators $\hat{a}_S$ and $\hat{a}_I$.

The equations of motion for the atomic operators are given by the Heisenberg-Langevin equations:

$$\frac{\partial}{\partial t}\hat{\sigma}_{ij} = \frac{i}{\hbar}[\hat{H}_{int}, \hat{\sigma}]_{ij} - \gamma_{ij}\hat{\sigma}_{ij} + \delta_{ij}\sum_l r_{li}\hat{\sigma}_{ll} + \hat{F}_{ij}, \quad (2)$$

where γ_{ij} are the decoherence rates, r_{li} are the spontaneous emission rates from $|l\rangle$ to $|i\rangle$ and $\hat{F}_{ij}$ are δ-correlated Langevin noise operators. The evolution of the fields is governed by the following propagation equations

$$\left(\frac{\partial}{\partial t} + c\frac{\partial}{\partial z}\right)\hat{a}_S = ig_S N\hat{\sigma}_{ge}, \quad (3)$$

$$\left(\frac{\partial}{\partial t} + c\frac{\partial}{\partial z}\right)\hat{a}_I = ig_I N\hat{\sigma}_{se'}. \quad (4)$$

We simplify these equations by assuming the signal and idler fields remain weak, such that they can be treated perturbatively in the atomic equations. This effectively fixes all of the population in the ground state. Therefore, the strong control field is not significantly depopulated and we can assume Ω and Ω′ are constant. We then adiabatically eliminate $|e'\rangle$ leaving four coupled equations:

$$i\partial_t\hat{\sigma}_{ge} = (\delta_s - \delta - i\gamma_{\text{ge}})\hat{\sigma}_{ge} - g\hat{a}_S + i\Omega\hat{\sigma}_{gs} + i\hat{F}_{ge}, \quad (5)$$

$$i\partial_t\hat{\sigma}_{gs} = (\delta_s - \delta - i\gamma_{\text{gs}})\hat{\sigma}_{gs} - g\frac{\Omega'}{\Delta}\hat{a}_I^\dagger - \Omega^*\hat{\sigma}_{ge} + i\hat{F}_{gs}, \quad (6)$$

$$(\partial_t + c\partial_z)\,\hat{a}_S = igN\hat{\sigma}_{ge}, \quad (7)$$

$$(\partial_t + c\partial_z)\,\hat{a}_I^\dagger = -igN\frac{\Omega'^*}{\Delta}\hat{\sigma}_{gs}, \quad (8)$$

where $\delta_S = |\Omega'|^2/\Delta$ is the AC-Stark shift and for simplicity we take $g_S = g_I = g$. The same equations can be derived directly from a 3-level model, as done by Phillips et al. [18], with the only difference being an additional AC-Stark shift in Eq.(5), $(\delta_s - \delta) \to (2\delta_s - \delta)$ that can not be removed by the choice of detunings. Since we are considering the far detuned regime with $\Delta \gg \gamma_{\text{ge}}$, this frequency shift δ_s can be neglected as it will be much smaller than the EIT transmission window.

III. PULSE PROPAGATION

In the case of constant control field we can easily solve Eqs.(5-8). For simplicity we take the single photon detuning to match the AC-Stark shift, $\delta = \delta_s = |\Omega|^2/\Delta$,

and set $\gamma_{\rm gs} = 0$. The solutions in terms of the optical depth D, are given in the frequency domain as:

$$\hat{a}_S(D,\omega) = A(D,\omega)\,\hat{a}_S(0,\omega) + B(D,\omega)\,\hat{a}_I^\dagger(0,-\omega) + \delta\hat{\alpha}_S, \tag{9}$$

$$\hat{a}_I^\dagger(D,\omega) = -B(D,\omega)\,\hat{a}_S(0,\omega) + C(D,\omega)\,\hat{a}_I^\dagger(0,-\omega) + \delta\hat{\alpha}_I. \tag{10}$$

The corresponding coefficients read:

$$A(D,\omega) = \left[\cosh\left(\frac{D\gamma_{\rm ge}U(\omega)}{2V(\omega)}\right) + \frac{\gamma_{\rm ge}|\epsilon|^2 - i\omega - i|\epsilon|^2\omega}{U(\omega)}\sinh\left(\frac{D\gamma_{\rm ge}U(\omega)}{2V(\omega)}\right)\right] e^{-\frac{D\gamma_{\rm ge}}{2V(\omega)}\left(i\omega - i\omega|\epsilon|^2 + |\epsilon|^2\gamma_{\rm ge}\right)}, \tag{11}$$

$$B(D,\omega) = -\frac{2i\epsilon\Omega}{U(\omega)}\sinh\left(\frac{D\gamma_{\rm ge}U(\omega)}{2V(\omega)}\right) e^{-\frac{D\gamma_{\rm ge}}{2V(\omega)}\left(i\omega - i\omega|\epsilon|^2 + |\epsilon|^2\gamma_{\rm ge}\right)}, \tag{12}$$

$$C(D,\omega) = \left[\cosh\left(\frac{D\gamma_{\rm ge}U(\omega)}{2V(\omega)}\right) - \frac{\gamma_{\rm ge}|\epsilon|^2 - i\omega - i|\epsilon|^2\omega}{U(\omega)}\sinh\left(\frac{D\gamma_{\rm ge}U(\omega)}{2V(\omega)}\right)\right] e^{-\frac{D\gamma_{\rm ge}}{2V(\omega)}\left(i\omega - i\omega|\epsilon|^2 + |\epsilon|^2\gamma_{\rm ge}\right)}, \tag{13}$$

where $\epsilon = \Omega'/\Delta$ defines the strength of 4WM, and:

$$U(\omega) = \sqrt{\left[i\omega + |\epsilon|^2(i\omega - \gamma_{\rm ge})\right]^2 + 4|\epsilon|^2|\Omega|^2}, \tag{14}$$

$$V(\omega) = \omega(\omega + i\gamma_{\rm ge}) - |\Omega|^2. \tag{15}$$

The terms $\delta\hat{\alpha}_S$ and $\delta\hat{\alpha}_I$ represent the field fluctuations corresponding to the Langevin noise operators. These can be neglected in the weak-field approximation since their normal ordered contributions are proportional to $\langle\hat{\sigma}_{ee}\rangle$ and $\langle\hat{\sigma}_{ss}\rangle$ respectively, which are second order in the signal field. However since these terms contribute to the noise, they will be considered in Sect. IV.

Another important quantity for EIT based QM is the matter excitation, since the light field is mapped onto it during the storage process. This excitation is described by the spin operator $\hat{\sigma}_{gs}$ which can be found in terms of Eqs.(9,10):

$$\hat{\sigma}_{gs}(D,\omega) = \frac{\Omega^* g}{V(\omega)}\left(\hat{a}_S(D,\omega) - \frac{\Omega'}{\Omega^*}\frac{\omega + i\gamma_{\rm ge}}{\Delta}\hat{a}_I^\dagger(D,\omega)\right). \tag{16}$$

It has contributions from both the signal and idler field, but the idler term is proportional to the small parameter $\gamma_{\rm ge}/\Delta$, and therefore can largely be ignored compared to the signal part. We can therefore concentrate on solving for the propagation of the signal field and our results will still be applicable to EIT quantum memory. Since we only consider propagation we ignore however any losses due to pulse leakage during the storing process.

The coefficients $A(D,\omega), C(D,\omega)$ describe the spectral transmission for the input signal and idler fields and the coefficient $B(D,\omega)$ describes the spectral coupling between the fields. Since we are mainly interested in quantum memory applications and it has already been shown that an input idler field is not stored [18], we will assume no input idler field, implying we can ignore $C(D,\omega)$. In this case, the semi-classical solution for the signal and idler fields are just:

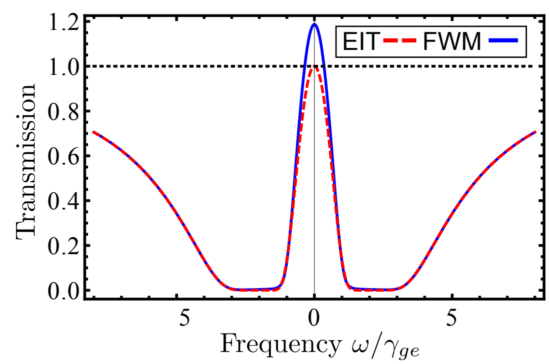

FIG. 2: Plot of the transmission coefficient as a function of frequency for EIT with 4WM (solid) and without 4WM (dashed). The parameters were chosen to emphasize the spectral behavior.

$$\alpha_S(D,\omega) \;=\; A(D,\omega)\,\alpha_S(0,\omega), \tag{17}$$

$$\alpha_I(D,\omega) \;=\; -B^*(D,\omega)\alpha_S^*(0,\omega). \tag{18}$$

While the expressions for A and B are complicated, in the limit of $\epsilon \ll 1$ which we have already assumed in order to derive the reduced Hamiltonian and $D > 1$ as is necessary for QM, both A and B are well approximated by Gaussians:

$$A(D,\omega) = A_0(D)e^{i\tau_S(D)\omega - \frac{\omega^2}{\Delta\omega_S^2}}, \tag{19}$$

$$B(D,\omega) = B_0(D)e^{i\tau_I(D)\omega - \frac{\omega^2}{\Delta\omega_I^2}}. \tag{20}$$

where the τ_S, τ_I are the group delay times for the signal and generated idler field, respectively; while $\Delta\omega_S$ and $\Delta\omega_I$ are the frequency widths. It is clear that amplitudes

A_0 and B_0 are the steady state solutions for the fields:

$$A_0 = \cosh\left(\frac{D\gamma_{\rm ge}\eta}{\Delta}\right) e^{\frac{D\gamma_{\rm ge}^2\eta^2}{2\Delta^2}} - \frac{i}{2}\frac{\eta\gamma_{\rm ge}}{\Delta}\sinh\left(\frac{D\gamma_{\rm ge}\eta}{\Delta}\right) e^{\frac{D\gamma_{\rm ge}^2\eta^2}{2\Delta^2}}, \tag{21}$$

$$B_0 = \frac{i\Omega'^*\Omega^*}{|\Omega'\Omega|}\sinh\left(\frac{D\eta\gamma_{\rm ge}}{\Delta}\right) e^{\frac{D\gamma_{\rm ge}^2\eta^2}{2\Delta^2}}. \tag{22}$$

We introduce the ratio of the control field Rabi frequencies $\eta = |\Omega'|/|\Omega|$, which only differs from unity when the two transitions have different dipole moments. It makes sense to introduce a parameter to keep track of the effective 4WM strength,

$$x = D\eta\frac{\gamma_{\rm ge}}{\Delta}. \tag{23}$$

Then for field propagation, Eqs.(21,22) defines two distinct regimes of x. For large 4WM strength $x > 1$, both the signal and idler field experience exponential growth and except for a phase factor are essentially the same amplitude, as shown in Fig. 3.

$$A_0 = \frac{1}{2}e^x, \tag{24}$$

$$B_0 = \frac{i}{2}\frac{\Omega'^*\Omega^*}{|\Omega'\Omega|}e^x. \tag{25}$$

At large optical depths the 4WM process is generating many more photons than in the initial pulse, and for every new signal field photon there is a corresponding idler photon generated. While for smaller optical depth, $x \ll 1$, there is only weak gain for the idler and signal field, i.e. we can treat this perturbatively:

$$A_0 = 1 + \frac{x^2}{2}, \tag{26}$$

$$B_0 = i\frac{\Omega'^*\Omega^*}{|\Omega'\Omega|}x. \tag{27}$$

The idler field grows faster than the signal, but since it starts from vacuum, it remains much weaker than the signal field. Since 4WM introduces gain on the signal field, which also leads to stronger matter excitations, when present it will always increase the classical storage and retrieval efficiencies for an EIT memory. Therefore, in experiments that see a loss of classical efficiencies at higher optical depths such as [16], the loss should not be attributed to 4WM, but rather to other processes that grow with optical depth such as increased dephasing or depletion of the control field. The case of particular interest for QM will be for small 4WM strengths $x < 1$, since we will show in Sect. IV that exponential growth of the signal field is accompanied by an equally strong growth in noise.

The group delay time for the fields is given by τ_S and τ_I, where a field traveling at the speed of light is taken

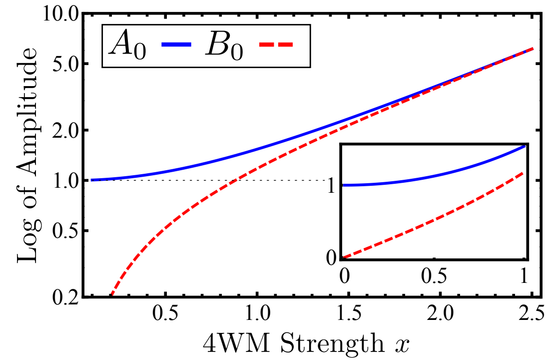

FIG. 3: Log plot of the signal (solid) and idler (dashed) amplitudes as a function of effective 4WM optical depth. Assuming no initial idler field and normalized to the amplitude of the initial signal field. Note both become equal and grow exponentially for high optical depths. The inset is a linear plot showing the the low optical depth behavior of the amplitudes.

not to have a time delay. In the low optical depth case:

$$\tau_S \simeq \frac{D\gamma_{\rm ge}}{|\Omega|^2}, \tag{28}$$

$$\tau_I \simeq \frac{D\gamma_{\rm ge}}{2|\Omega|^2}, \tag{29}$$

such that τ_S is essentially the standard EIT delay time. The delay time for the generated idler τ_I, is approximately half of that for the signal field. This can be understood as a consequence of the idler field being generated from the signal field. While the idler field is essentially moving at the speed of light and therefore is not delayed, it is also constantly being generated by the slow signal field. The total delay time is then the average of delay for idler photons generated near the beginning of the medium, and the idler photons generated at the end of the medium after the slower signal field has traversed the medium length. A similar effect is seen at high optical depth:

$$\tau_S \simeq \tau_I \simeq \frac{D\gamma_{\rm ge}}{2|\Omega|^2}, \tag{30}$$

where there is now a locking of the velocities for both fields to the average. Both fields are growing exponentially and travel together, the faster idler field is generating a new slower signal field which leads to less signal delay, while the slower signal field generates the idler field leading to a longer idler delay than the low optical depth case.

The spectral behavior of the fields described by the frequency widths $\Delta\omega_S$ and $\Delta\omega_I$, and we can again distinguish between two different regimes. For low optical

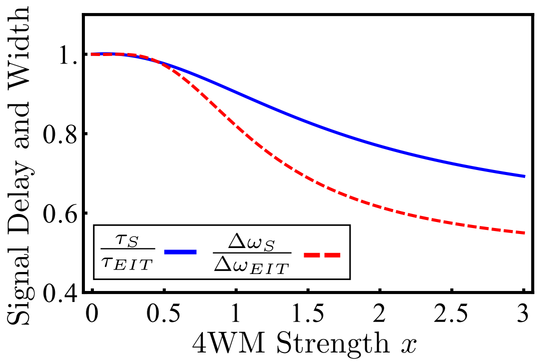

FIG. 4: Plot of the signal delay time, normalized to the standard EIT delay time $D\gamma_{\rm ge}/|\Omega|^2$ (solid) and the signal transmission frequency width, normalized to the standard EIT transmission window $|\Omega|^2/(\gamma_{\rm ge}\sqrt{D})$ (dashed), as a function of the effective 4WM optical depth.

depth,

$$\Delta\omega_S \simeq \frac{|\Omega|^2}{\gamma_{\rm ge}\sqrt{D}}, \tag{31}$$

$$\Delta\omega_I \simeq \frac{|\Omega|^2}{\gamma_{\rm ge}\sqrt{D}}\sqrt{\frac{2}{1+D/12}}. \tag{32}$$

Where $\Delta\omega_S$ defines the usual EIT transmission window with a small correction, and $\Delta\omega_I$ defines a larger window of transparency since the idler field does not experience absorption. At high optical depth:

$$\Delta\omega_S \simeq \Delta\omega_I \simeq \frac{|\Omega|^2}{\gamma_{\rm ge}\sqrt{D}}\sqrt{\frac{8\gamma_{\rm ge}\eta}{\Delta}}. \tag{33}$$

The fields are now propagating together with a similar transmission window that is narrower than the original EIT transmission window by a factor of $\sqrt{8\gamma_{\rm ge}/\Delta}$. This narrowing is due to preferential gain of the signal near resonance where it does not experience absorption, rather than at frequencies near the edge of the EIT transmission window that see some absorption. We have shown that for low optical depth $D < |\Delta|/\gamma_{\rm ge}$, the signal field propagates similar to normal EIT, with a small gain due to 4WM from the newly generated idler field which remains weak compared to the signal field and propagates through the medium as if it was transparent. The propagation is dramatically different at high optical depths $D > |\Delta|/\gamma_{\rm ge}$, where exponential growth of the signal and idler field couple the fields such that they have equal amplitudes, experience less group delay, and have a narrower transmission window.

IV. SIGNAL INTENSITY AND ADDITIVE PHOTON NOISE

As an indicative measure for the effect of 4WM on light storage in an EIT medium we now consider the number

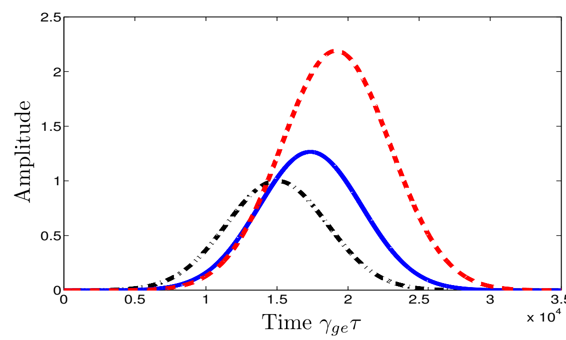

FIG. 5: Plot of the signal field at the beginning of the medium (dot-dashed), after an effective optical depth of $x = .75$ (solid), and after $x = 3$ (dashed). Normalized to the initial pulse amplitude.

of signal photons at the end of the medium at some time τ using Eqs.(9,10):

$$\begin{aligned}\langle \hat{a}_S^\dagger(D,\tau)\hat{a}_S(D,\tau)\rangle &= \iint \mathrm{d}\omega'\mathrm{d}\omega\, e^{-i(\omega'-\omega)\tau}\Big[\langle A^*(D,\omega')\hat{a}_S^\dagger(0,\omega')A(D,\omega)\hat{a}_S(0,\omega)\rangle \\ &\quad + \langle B^*(D,\omega')\hat{a}_I(D,\omega')B(D,\omega)\hat{a}_I^\dagger(D,\omega)\rangle\Big] \end{aligned} \tag{34}$$

$$= \iint \mathrm{d}\omega'\mathrm{d}\omega e^{-i(\omega'-\omega)\tau}\,\langle A^*(D,\omega')\hat{a}_S^\dagger(0,\omega')A(D,\omega)\hat{a}_S(0,\omega)\rangle + \int d\omega|B(D,\omega)|^2, \tag{35}$$

where the first part corresponds to the semi-classical solution, which one would obtain by treating the fields classically with no input idler field. For the second part we used the commutator relation for the field operators $[\hat{a}_I(\omega'),\hat{a}_I^\dagger(\omega)] = \delta(\omega-\omega')$, i.e. this part is a pure quantum mechanical effect which does not appear in the semi-classical solution. Since the value of the second part is equal for all time τ it describes the generation rate of the incoherent signal photons. This contribution exists even

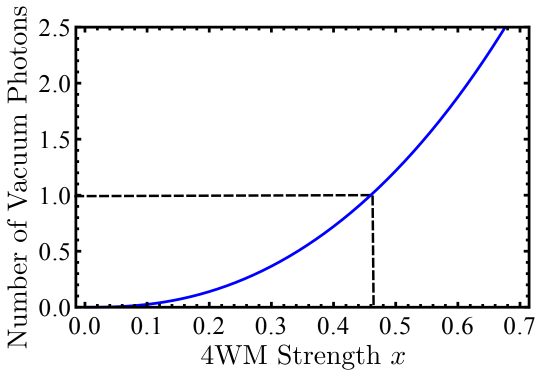

FIG. 6: Plot of the number of noise photons produced as a function of effective 4WM optical depth. Notice it becomes larger than 1 slightly before when $D > \Delta/(2\gamma_{\rm ge})$.

when there is no field input at all, and therefore is important for few photon input fields consequently, we refer to this as the vacuum noise contribution. It does not grow with signal field strength, so is much less important for fields with large photon number. With this we are able to estimate the number of noise photos by multiplying the generation rate with the propagation time of the signal field. As noted in Sect. III, at high optical depth $x > 1$, A_0 and B_0 are equal, which implies that for a single photon input, the vacuum noise contribution will be as strong as the output of the signal field. Therefore in the regime of $x > 1$, a quantum memory is impossible. And as one can see from the graph in Fig.6 we get additional noise photons even for 4WM strengths not much larger than .5.

V. FIDELITY OF PROPAGATION

For a wave propagating through our medium, we can calculate the fidelity by finding the overlap of the wave-function well before the medium and the wave-function well after leaving the medium.

$$F_{|\Psi_{\rm in}\rangle} = \sqrt{\langle\Psi_{\rm in}|\,\rho_{\rm out}\,|\Psi_{\rm in}\rangle}. \tag{36}$$

To describe propagation we consider a quantization length L_Q much longer than the medium, which we subdivide into $2M+1$ spatial intervals, each with center point:

$$z_n = \frac{nL_Q}{2M+1}, \tag{37}$$

with n running from $-M$ to M. To describe a field pulse we also must divide frequency into $2M+1$ discrete modes, centered at the resonance frequencies. We want to have two creation operators, one that creates a signal field photon of frequency ω_n given by $\hat{c}_n$, and one that creates an idler photon given by $\hat{b}_n$, such that:

$$\hat{c}_n^\dagger\,|\{0\}\rangle_S = |1_n\rangle_S \prod_{p\neq n} |0_p\rangle_S \tag{38}$$

$$\hat{b}_n^\dagger\,|\{0\}\rangle_I = |1_n\rangle_I \prod_{p\neq n} |0_p\rangle_I \tag{39}$$

where we are labeling the vacuum for the signal and idler field as:

$$|\{0\}\rangle_S = \prod_n |0_n\rangle_S \tag{40}$$

$$|\{0\}\rangle_I = \prod_n |0_n\rangle_I \tag{41}$$

Then the field annihilation operator for the signal or idler field at a particular z_l are described by:

$$\hat{a}_{S,l} = \frac{1}{\sqrt{2M+1}} \sum_{n=-M}^{M} \hat{c}_{l,n} \exp\left(\frac{2\pi i n l}{2M+1}\right), \tag{42}$$

$$\hat{a}_{I,l} = \frac{1}{\sqrt{2M+1}} \sum_{n=-M}^{M} \hat{b}_{l,n} \exp\left(\frac{2\pi i n l}{2M+1}\right). \tag{43}$$

With the medium centered inside the quantization length, it begins at some z_q and ends at $z_{q'}$. Since when not in the medium the field is freely propagating, all we need to know is how it changes within the medium. Eq.(9) gives an input-output relation for each frequency ω_n:

$$\hat{c}_{q',n} = A_n \hat{c}_{q,n} + B_n \hat{b}_{q,n}^\dagger, \tag{44}$$

which we can use to find the normal ordered characteristic function χ_N for a particular input state. The characteristic function in turn is the complex Fourier-transform of the multi-mode Glauber P-representation, from which we can easily determine the overlap in Eq.(36) defining the fidelity.

We are particularly interested in the input of a single photon state in the signal channel, which we represent as:

$$|\Psi_{\rm SP}\rangle = |\{1\}\rangle = \sum_{i=-M}^{M} f_i\,\hat{c}_i^\dagger\,|\{0\}_S\rangle\,|\{0\}_I\rangle, \tag{45}$$

where f_i is a distribution function that represents the photons frequency envelope, and is normalized to produce a single photon by:

$$\sum_{i=-M}^{M} |f_i|^2 = 1. \tag{46}$$

After some straight-forward algebra we can then write the fidelity for a single photon input state as an integral:

$$F_{\rm SP}^2 = \prod_{n=-M}^{M} \frac{1}{\pi^2} \int_{-\infty}^{\infty} d\beta_n^2 \int_{-\infty}^{\infty} d\eta_n^2 |\langle\{1\}|\{\beta\}\rangle|^2 e^{\eta_n^*\beta_n - \eta_n\beta_n^*}\chi_N \tag{47}$$

where $|\langle\{1\}|\{\beta\}\rangle|^2$ is the overlap of the single photon state with the multimode coherent state:

$$|\langle\{1\}|\{\beta\}\rangle|^2 = (\prod_n e^{-|\beta_n|^2})(\sum_{j,k} f_j^* f_k \beta_j \beta_k^*), \tag{48}$$

and χ_N is the normally ordered characteristic function at the output of the medium which can be expressed in terms of the solutions of the Heisenberg equations of motion for the field operators:

$$\chi_N = \langle\Psi_{\mathrm{SP}}|\, \exp\left(+\sum_{n=-M}^{M} \frac{\eta_n}{\sqrt{2M+1}}\hat{c}^\dagger_{q',n}\right) \exp\left(-\sum_{m=-M}^{M} \frac{\eta_m^*}{\sqrt{2M+1}}\hat{c}_{q',m}\right) |\Psi_{\mathrm{SP}}\rangle. \tag{49}$$

Now using Eq.(44) we get an expectation value that we can solve, in particular we can break the problem into finding the contribution from the signal field and the vacuum contribution from the idler:

$$\chi_N = \chi_N^{\mathrm{sig}}\chi_N^{\mathrm{vac}}, \tag{50}$$

with:

$$\chi_N^{\mathrm{sig}} = 1 - \sum_{n,m} f_n^* f_m \frac{\eta_n A_n^* \eta_m^* A_m}{2M+1}, \tag{51}$$

$$\chi_N^{\mathrm{vac}} = \exp\left(-\sum_n \frac{|\eta_n|^2|B_n|^2}{2M+1}\right). \tag{52}$$

Performing the integrals while being careful with the sums gives the single photon fidelity as:

$$F_{\mathrm{SP}}^2 = \left(\prod_{n=-M}^{M} \frac{1}{1+\frac{|B_n|^2}{2M+1}}\right)\left[\sum_{i,j} \frac{|f_i|^2|f_j|^2\frac{A_i^* A_j}{2M+1}}{(1+\frac{|B_i|^2}{2M+1})(1+\frac{|B_j|^2}{2M+1})} + \sum_i \frac{|f_i|^2\frac{|B_i|^2}{2M+1}}{(1+\frac{|B_i|^2}{2M+1})} - \sum_{i,j} \frac{|f_i|^2|f_j|^2\frac{|A_i|^2}{2M+1}\frac{|B_j|^2}{2M+1}}{(1+\frac{|B_i|^2}{2M+1})(1+\frac{|B_j|^2}{2M+1})}\right] \tag{53}$$

Eq.(53) has two parts, a product multiplied by a sum. The product can be interpreted as the vacuum contribution, it is the same as would be calculated for a vacuum state. It always converges and depends on the spectral width of the coupling coefficient. In the continuous limit it can be explicitly calculated:

$$\prod_{n=-M}^{M} \frac{1}{1+\frac{|B_n|^2}{2M+1}} \to \exp\left(-\frac{\tau_S}{2}\int_{-\infty}^{\infty} d\omega |B(D,\omega)|^2\right). \tag{54}$$

For large optical depths $|B_0|^2 \gg 1$, this term dominates the single photon fidelity quickly dropping it to zero, with a rate that is at least exponential in optical depth. The second part is given by the sums in Eq.(53), and is due to the gain on the signal field; in the continuum limit $M \to \infty$ can be converted back into integrals:

$$\sum_i \frac{|f_i|^2\frac{A_i^*}{\sqrt{2M+1}}}{(1+\frac{|B_i|^2}{2M+1})} \to \int_{-\infty}^{+\infty} d\omega |f(\omega)|^2 \frac{A^*(\omega)}{(1+|B(\omega)|^2)}$$
$$\simeq \frac{A_0^*}{1+|B_0|^2}\sqrt{\frac{1}{1+\frac{\Delta\omega_0^2}{\Delta\omega_S^2} - 2\frac{|B_0|^2}{1+|B_0|^2}\frac{\Delta\omega_0^2}{\Delta\omega_I^2}}}\exp\left(-\frac{\tau_S^2\Delta\omega_0^2}{4}\frac{1}{1+\frac{|B_0|^2}{1+|B_0|^2}\frac{\Delta\omega_0^2}{\Delta\omega_I^2}}\right), \tag{55}$$

$$\sum_i \frac{|f_i|^2\frac{|A_i|^2}{\sqrt{2M+1}}}{(1+\frac{|B_i|^2}{2M+1})} \to \int_{-\infty}^{+\infty} d\omega |f(\omega)|^2 \frac{|A(\omega)|^2}{(1+|B(\omega)|^2)} \simeq \frac{|A_0|^2}{1+|B_0|^2}\sqrt{\frac{1}{1+2\frac{\Delta\omega_0^2}{\Delta\omega_S^2} - 2\frac{|B_0|^2}{1+|B_0|^2}\frac{\Delta\omega_0^2}{\Delta\omega_I^2}}}, \tag{56}$$

$$\sum_j \frac{|f_j|^2\frac{|B_j|^2}{\sqrt{2M+1}}}{(1+\frac{|B_j|^2}{2M+1})} \to \int_{-\infty}^{+\infty} d\omega |f(\omega)|^2 \frac{|B(\omega)|^2}{(1+|B(\omega)|^2)} \simeq \frac{|B_0|^2}{1+|B_0|^2}\sqrt{\frac{1}{1+\frac{1-|B_0|^2}{1+|B_0|^2}\frac{\Delta\omega_0^2}{\Delta\omega_I^2}}}. \tag{57}$$

Where we have assumed that all the functions are Gaussians given by Eqs.(19, 20) and our initial distribution

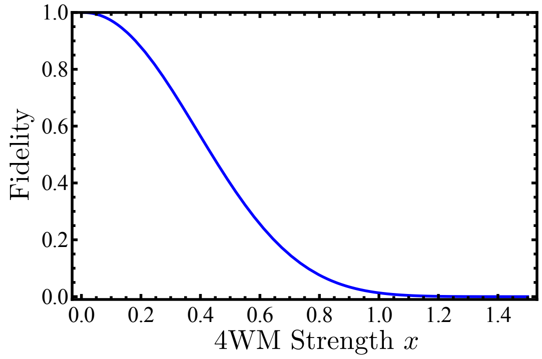

FIG. 7: Plot of fidelity for the single photon case as a function of the effective 4WM optical depth. In the limit $\Delta_0/\Delta\omega_S, \Delta\omega_0/\Delta\omega_I \to 0$.

function is a Gaussian such that:

$$|f(\omega)|^2 = \frac{1}{\sqrt{\pi}\Delta\omega_0} e^{-(\frac{\omega}{\Delta\omega_0})^2}, \tag{58}$$

where $\Delta\omega_0$ is the frequency width of the incoming pulse.

Now lets consider the ideal case where the frequency width of the incoming pulse fits well inside the transmission window and define this ratio as y:

$$\frac{\Delta\omega_0}{\Delta\omega_S} \ll \sqrt{\frac{2}{D}}, \tag{59}$$

where we have chosen this limit such that the exponential term in Eq.(55) can be dropped. Then consider two different limits for the 4WM strength, for $x > 1$ the fidelity exponentially decreases, while for small x and keeping only the first order terms we can express the fidelity as:

$$F_{\text{SP}} = \exp\left(-\sqrt{3}D\frac{|\Omega'|^2}{\Delta^2}\right)\sqrt{1 - \frac{\Delta\omega_0^2}{\Delta\omega_S^2} - x^2}. \tag{60}$$

This shows us that the single photon fidelity will always be worse due to 4WM, although this is the expected result since without 4WM, we have standard EIT, which for narrow pulse spectrum has fidelity close to 1. Therefore when 4WM is unavoidable, it would be best to implement quantum memory in the regime $D < \Delta/\gamma_{\text{ge}}$, which can be accomplished by choosing a medium with small γ_{ge}, such as picking a low temperature implementation like a cold Rubidium gas trapped in a magneto-optical trap, rather than a warm gas cell.

VI. FIDELITY OF PROPAGATION WITH LOSSES

As we have seen in the previous section, the presence of gain due to 4WM leads to a fast reduction of fidelity in otherwise loss-less propagation. We now analyze if 4WM could be beneficial when there are some linear losses due to scattering in the medium. We consider in particular the case where the 4WM gain exactly compensates linear loss, for which we will compare the EIT and 4WM single photon fidelities.

Our analysis in Sect.V also applies to EIT in the limit of $A_0 \to 1$ and $B_0 \to 0$. In order to model linear losses in EIT with spatial loss coefficient λ we just need to take the expression for the single photon fidelity and replace the coefficients with $A_0 = \exp(-\lambda D/2)$ and $B_0 = 0$. In that limit the only integral needed is much simpler with:

$$\int_{-\infty}^{\infty} d\omega |f(\omega)|^2 A(\omega) = A_0\sqrt{\frac{\Delta\omega_S^2}{\Delta\omega_0^2 + \Delta\omega_S^2}} \exp\left(-\frac{\Delta\omega_0^2\Delta\omega_S^2}{4(\Delta\omega_0^2 + \Delta\omega_S^2)}\tau_S^2\right), \tag{61}$$

which in the limit of $\Delta\omega_0/\Delta\omega_S \ll \sqrt{2/D}$, collapses the fidelity of EIT with losses to the expected result of:

$$F_{\text{SP}}^{\text{EIT}} \simeq |A_0|^2 = e^{-\lambda D}. \tag{62}$$

The same loss can be added to the 4WM fidelity by taking $A_0 \to A_0 \exp(-\lambda D/2)$ and $B_0 \to B_0 \exp(-\lambda D/2)$.

We pose the question of when does the 4WM single photon fidelity surpass that of the the EIT, assuming both systems experience linear loss. In the limit of $\Delta\omega_0/\Delta\omega_S \to 0$, we can approximate the fidelity as:

$$F_{\text{SP}} = \left[\frac{|A_0|^2(1 - |B_0|^2)}{(1 + |B_0|^2)^2} + \frac{|B_0|^2}{1 + |B_0|^2}\right] e^{-\frac{\tau_S}{2}\Delta\omega_I |B_0|^2} \tag{63}$$

Now we can take the steady state solution $|A_0|^2 = q\cosh^2(x)$ and $|B_0|^2 = q\sinh^2(x)$, with the EIT fidelity given by $q = \exp(-\lambda D)$. In this case it is fairly simple to calculate when 4WM can improve over EIT, it is possible when $q \leq .5$, i.e. the EIT fidelity is already less than .5, as illustrated in Fig. 8. So while 4WM can be an improvement, it only helps in cases where the fidelity is already too bad to use as a quantum memory.

VII. NOISE DUE TO FINITE EXCITED STATE POPULATION

There will also be noise contributions due to spontaneous emission, which we previously neglected since contributions from the Langevin noise operators are second order in the signal or idler fields. In the following we will calculate these noise contributions. The noise operators introduced in Eqs.(9,10) read explicitly:

$$\delta\hat{\alpha}_S(\xi,\omega) = \int_0^{\xi} d\xi' A(\xi - \xi',\omega)\hat{F}_S + \int_0^{\xi} d\xi' B(\xi - \xi',\omega)\hat{F}_I, \tag{64}$$

$$\delta\hat{\alpha}_I(\xi,\omega) = -\int_0^{\xi} d\xi' B(\xi - \xi',\omega)\hat{F}_S + \int_0^{\xi} d\xi' C(\xi - \xi',\omega)\hat{F}_I, \tag{65}$$

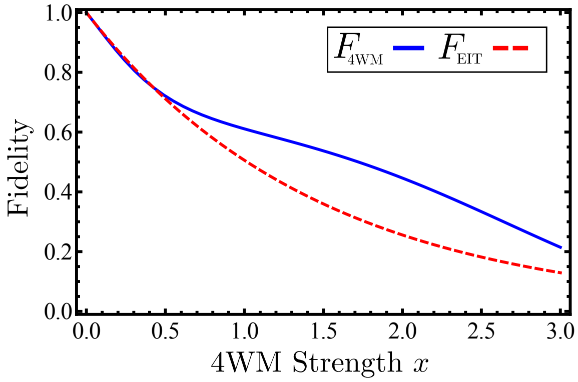

FIG. 8: Plot of fidelity of four wave mixing (solid) and standard EIT (dashed) fidelities as a function of effective optical depth in the presence of linear losses, under the assumption that the signal field is always well within the transmission window. The losses are taken to match the 4WM gain present at the effective optical depth of 2, and with $\gamma_{\rm ge}\eta/\Delta = 1/30$.

where A, B, and C are given by Eqs.(11-13), and the new $\hat{F}$ operators are defined in terms of the Langevin noise operators:

$$\begin{aligned} \hat{F}_S =& \frac{gN\Omega}{(\omega+i\gamma_{gs})(\omega+i\gamma_{ge})-|\Omega|^2}\hat{F}_{gs} \\ &- \frac{gN(\omega+i\gamma_{gs})}{(\omega+i\gamma_{gs})(\omega+i\gamma_{ge})-|\Omega|^2}\hat{F}_{ge} \qquad (66) \\ \hat{F}_I =& \frac{gN\Omega'^*(\omega+i\gamma_{\rm ge})/\Delta}{(\omega+i\gamma_{gs})(\omega+i\gamma_{ge})-|\Omega|^2}\hat{F}_{gs} \\ &- \frac{gN\Omega^*\Omega'^*/\Delta}{(\omega+i\gamma_{gs})(\omega+i\gamma_{ge})-|\Omega|^2}\hat{F}_{ge} \qquad (67) \end{aligned}$$

The rate of generation for extra amplitude noise due to spontaneous emission, is given by the expectation value $\langle\delta\hat{\alpha}_S^\dagger\delta\hat{\alpha}_S\rangle$ for which to the first non-zero order in Ω'/Δ is:

$$\langle\delta\hat{\alpha}_S^\dagger\delta\hat{\alpha}_S\rangle = \frac{1}{2\pi}\int_{-\infty}^{\infty}d\omega\int_{-\infty}^{\infty}d\omega'\int_0^D d\xi\int_0^D d\xi' A^*(D-\xi,\omega)A(D-\xi',\omega')\langle\hat{F}_S^\dagger(\xi,\omega)\hat{F}_S(\xi',\omega')\rangle e^{i(\omega-\omega')t}. \qquad (68)$$

While the form of the $\hat{F}$ are unknown, their expectations can be calculated using the fluctuation dissipation theorem [20], but we need to consider the full set of equations from the reduced Hamiltonian given in Eq.(1), not just the $\sigma_{\rm ge}$ and $\sigma_{\rm gs}$ equations Eqs.(5,6). The full equations, neglecting detunings, letting $\gamma_{\rm gs}=0$, and dropping terms that are third power in the fields are:

$$\dot{\hat{\sigma}}_{ge} = i\omega\hat{\sigma}_{ge} - \gamma_{\rm ge}\hat{\sigma}_{ge} + ig\hat{a}_S + i\Omega\hat{\sigma}_{gs} + \hat{F}_{ge}, \qquad (69)$$

$$\dot{\hat{\sigma}}_{se} = -\gamma_{\rm se}\hat{\sigma}_{se} + i\Omega(\hat{\sigma}_{ss}-\hat{\sigma}_{ee}) - i\frac{\Omega'^*g\hat{a}_I}{\Delta}\hat{\sigma}_{ge} + ig\hat{a}_S\hat{\sigma}_{gs}^\dagger + \hat{F}_{se}, \qquad (70)$$

$$\dot{\hat{\sigma}}_{gs} = i\omega\hat{\sigma}_{gs} + i\frac{\Omega' g\hat{a}_I^*}{\Delta} + i\Omega^*\hat{\sigma}_{ge} + \hat{F}_{gs}, \qquad (71)$$

$$\dot{\hat{\sigma}}_{ee} = -r_{es}\hat{\sigma}_{ee} - r_{eg}\hat{\sigma}_{ee} - ig\hat{a}_S^\dagger\hat{\sigma}_{ge} + ig\hat{a}_S\hat{\sigma}_{ge}^\dagger - i\Omega^*\hat{\sigma}_{se} + i\Omega\hat{\sigma}_{se}^\dagger + \hat{F}_{ee}, \qquad (72)$$

$$\dot{\hat{\sigma}}_{ss} = r_{es}\hat{\sigma}_{ee} - r_{sg}\hat{\sigma}_{ss} - i\frac{\Omega'^*}{\Delta}g\hat{a}_I^{\dagger *}\hat{\sigma}_{gs} + i\frac{\Omega'}{\Delta}g\hat{a}_I^*\hat{\sigma}_{gs}^\dagger + i\Omega^*\hat{\sigma}_{se} - i\Omega\hat{\sigma}_{se}^\dagger + \hat{F}_{ss}. \qquad (73)$$

Notice that the equations are no longer linear, but we expect the noise term to be second order in the fields. From Eqs.(70-73) we can find the expectation values for the Langevin noise operators:

$$\langle\hat{F}_{ge}^\dagger\hat{F}_{ge}\rangle = (2\gamma_{\rm ge} - r_{es} - r_{eg})\langle\hat{\sigma}_{ee}\rangle, \qquad (74)$$

$$\langle\hat{F}_{gs}^\dagger\hat{F}_{gs}\rangle = r_{es}\langle\hat{\sigma}_{ee}\rangle, \qquad (75)$$

$$\langle\hat{F}_{ge}^\dagger\hat{F}_{gs}\rangle = (\gamma_{\rm ge} - \gamma_{\rm se})\langle\hat{\sigma}_{se}^\dagger\rangle, \qquad (76)$$

$$\langle\hat{F}_{gs}^\dagger\hat{F}_{ge}\rangle = (\gamma_{\rm ge} - \gamma_{\rm se})\langle\hat{\sigma}_{se}\rangle. \qquad (77)$$

Now with these expectation values we can calculate $\langle\hat{F}_S^\dagger\hat{F}_S\rangle$:

$$\begin{aligned} \langle\hat{F}_S^\dagger(\xi,\omega)\hat{F}_S(\xi',\omega')\rangle =& \frac{g^2N^2}{|\omega(\omega-i\gamma_{\rm ge})-|\Omega|^2|^2}\Big[\\ & r_{es}|\Omega|^2\langle\hat{\sigma}_{ee}\rangle + (\gamma_{\rm se}-\gamma_{\rm ge})\langle\hat{\sigma}_{se}\rangle\omega\Omega^* + (\gamma_{\rm se}-\gamma_{\rm ge})\langle\hat{\sigma}_{se}^\dagger\rangle\omega\Omega \\ & + \omega^2(2\gamma_{\rm ge}-r_{es}-r_{eg})\langle\hat{\sigma}_{ee}\rangle)\delta(\xi-\xi')\Big]\delta(\omega-\omega'). \qquad (78) \end{aligned}$$

The expectation values of the atomic operators can be found in terms of the field expectations by solving Eqs.(70-73), in the limit $|\gamma_{\rm se}-\gamma_{\rm ge}| \ll \gamma_{\rm se}$ the $\langle\hat{\sigma}_{se}\rangle$ can be neglected. Then only the excited state population is important. We can further simplify by assuming

$\omega \ll \gamma_{\rm ge}, \gamma_{\rm se}$, since this term is multiplied by the $A(\omega)$ which vanishes for frequencies outside the EIT width, then the average excited state population can be found by solving the semi-classical form of Eqs.(70-73):

$$\langle\hat{\sigma}_{ee}\rangle = \frac{2g^2\gamma_{\rm ge}\omega^2\alpha_S^*\alpha_S}{r_{eg}|V(\omega)|^2} - \frac{2g^2\gamma_{\rm ge}\omega(|\Omega'\Omega|/\Delta)\sqrt{|\alpha_S\alpha_I|}}{r_{eg}|V(\omega)|^2} + \frac{2g^2\gamma_{\rm ge}|\Omega|^2(|\Omega'|^2/\Delta^2)\alpha_I\alpha_I^*}{r_{eg}|V(\omega)|^2}, \tag{79}$$

where α_S and α_I are the semi-classical field solutions given by Eqs.(17,18). Replacing the initial field expectation value with the distribution given by Eq.(58) and multiplying by the delay time of the signal field τ_D yields the number of noise photons affected by dephasing due to spontaneous emission:

$$\mathcal{N}_{\rm SE} = \tau_D\langle\delta\hat{\alpha}_S^\dagger\delta\hat{\alpha}_S\rangle = \tau_D\int_{-\infty}^{\infty}\mathrm{d}\omega\int_0^D \mathrm{d}\xi|A(D-\xi,\omega)|^2|f(\omega)|^2\frac{g^4N^2[(2\gamma_{\rm ge}-r_{es}-r_{eg})\omega^2+r_{es}|\Omega|^2]}{r_{eg}[\gamma_{\rm ge}^2\omega^2+|\Omega|^4]^2}$$
$$\times\left[2\gamma_{\rm ge}\omega^2|A(\xi,\omega)|^2 - 2\gamma_{\rm ge}\omega\frac{|\Omega'\Omega|}{\Delta}|A(\xi,\omega)||B(\xi,\omega)| + 2\gamma_{\rm ge}|\Omega|^2\frac{|\Omega'|^2}{\Delta^2}|B(\xi,\omega)|^2\right]. \tag{80}$$

The integral over ξ is straight forward when we use the Gaussian approximation developed in Sect. III for $A(\xi,\omega)$ and $B(\xi,\omega)$. Approximating $|A_0(\xi)| = \cosh(\gamma_{\rm ge}\eta\xi/\Delta)$ and $|B_0(\xi)| = \sinh(\gamma_{\rm ge}\eta\xi/\Delta)$, and performing the ξ integral leaves us with:

$$\mathcal{N}_{\rm SE} = \tau_D\int_{-\infty}^{\infty} d\omega e^{-2(\omega/\Delta\omega_S)^2}|f(\omega)|^2\frac{g^2N^2[(2\gamma_{\rm ge}-r_{es}-r_{eg})\omega^2+r_{es}|\Omega|^2]}{r_{eg}[\gamma_{\rm ge}^2\omega^2+|\Omega|^4]^2}$$
$$\times\Bigg[2\gamma_{\rm ge}\omega^2e^{-2(\omega/\Delta\omega_S)^2}\Big(-\frac{D}{4}+\frac{D}{8}\cosh(x)+\frac{5D}{16x}\sinh(2x)\Big)$$
$$-2\gamma_{\rm ge}\omega\frac{|\Omega'\Omega|}{\Delta}e^{-(\omega/\Delta\omega_S)^2}e^{-(\omega/\Delta\omega_I)^2}\sinh(x)\Big(\frac{D}{4}\cosh(x)+\frac{1}{4}\sinh(x)\Big)$$
$$+2\gamma_{\rm ge}|\Omega|^2\frac{|\Omega'|^2}{\Delta^2}e^{-2(\omega/\Delta\omega_I)^2}\Big(-\frac{D}{4}+\frac{D}{8}\cosh(2x)+\frac{D}{16x}\sinh(2x)\Big)\Bigg] \tag{81}$$

Now consider that the spectral window of $A(D,\omega)$ will ensure that the main contribution of the integral comes for small ω, so we can take $\omega < |\Omega|^2/\gamma_{\rm ge}$. This will allow us to approximate by replacing $\gamma_{\rm ge}^2\omega^2 + |\Omega|^4$ with $|\Omega|^4$ and perform the ω integral:

$$\mathcal{N}_{\rm SE} \simeq \frac{g^4N^2r_{es}\tau_D}{r_{eg}|\Omega|^6}\frac{D}{4}\left[\Delta\omega_0^2\gamma_{\rm ge}\Big(\frac{1}{2}\cosh(x)-1+\frac{5}{4x}\sinh(2x)\Big)+\gamma_{\rm ge}|\Omega|^2\frac{|\Omega'|^2}{\Delta^2}\Big(\cosh(2x)-2+\frac{1}{2x}\sinh(2x)\Big)\right] \tag{82}$$

This can be simplified by taking $r_{es} = r_{eg}$, and by noticing that the square of the group index $n_g^2 = g^4N^2/|\Omega|^2$ is approximately equal to $1/(\gamma_{\rm ge}\tau_D)$. Assuming first that we are in the small optical depth regime, where $x < 1$, we can simplify further:

$$\mathcal{N}_{\rm SE} \simeq \frac{D}{2}\left[\frac{\Delta\omega_0^2}{|\Omega|^2}(1+\frac{x^2}{8})+\frac{|\Omega'|^2}{\Delta^2}(\frac{1}{2}+x^2)\right]. \tag{83}$$

We can also consider the case when the optical depth is large $x \gg 1$, then we have:

$$\mathcal{N}_{\rm SE} \simeq \frac{D}{16}e^{2x}\left[\frac{\Delta\omega_0^2}{|\Omega|^2}\frac{5}{2x}+2\frac{|\Omega'|^2}{\Delta^2}\right], \tag{84}$$

which like the vacuum noise is exponentially growing. It is important to note that the noise induced by spontaneous emission is proportional to the initial signal field strength, and as shown in Fig. 9 for a small number of initial photons its contribution will be much weaker than the vacuum noise contribution given in Sect. IV. Therefore our dropping of this effect in the fidelity calculation of Sect. V is justified. Of course for a classical field with a large number of photons, dephasing due to spontaneous emission will be the dominate contribution to the noise.

VIII. CONCLUSION

We developed a model for a field propagating inside an EIT medium that has 4WM. We found that there are limits on the use of 4WM EIT as a single photon quantum memory based just on the propagation fidelity. There are two sources of noise, first we identified a 4WM

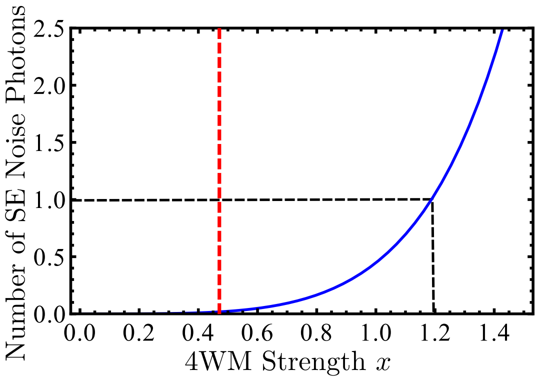

FIG. 9: Number of photons affected by spontaneous emission showing at what effective 4WM optical depth it becomes larger than 1, assuming a single photon input. For comparison the vertical dashed line shows the effective 4WM optical depth when the vacuum noise becomes 1.

process that creates new signal photons from the vacuum. The second source comes from the finite population that 4WM adds to the excited state, leading to dephasing of the dipoles due to spontaneous emission. Together both sources of noise become exponentially large for optical depths $D > \Delta|\Omega'|/(\gamma_{\rm ge}|\Omega|)$. This gives a natural limit on how high optical depth can be in EIT based quantum memories when 4WM is present.

We further show that even in the best case scenario where the gain from 4WM compensates some natural losses in the system, for example due to scattering, the propagation fidelity of 4WM EIT is still worse than that for standard EIT unless the EIT fidelity is below one half. Therefore for an EIT quantum memory, it is always preferential to avoid four-wave mixing. This can be accomplished by either choosing proper polarizations such that the control field can not couple to the signal transition, or by keeping the optical depth below the limit $D < \Delta/\gamma_{\rm ge}$. Since high optical depth is needed for an efficient quantum memory, this limit for D is easier to accomplish in systems with smaller $\gamma_{\rm ge}$, such as cold gas based memories rather than those in hot gas where the ratio of $\Delta/\gamma_{\rm ge}$ is much smaller.

Our model is limited by only considering propagation of the field through the medium, this ignores the fact that it is actually the collective spin excitation that gets stored in an EIT memory. Our approach also neglects considering the limits imposed by needing the field to be wholly within the EIT medium at the point where the field would be turned off for EIT storage. While considering these effects would not improve the limit 4WM imposes on the optical depth, it is possible that when considering the fidelity of the spin wave and the limits on the pulse length, that there are scenarios for lower optical depths where 4WM could be useful. We plan to further investigate the effect of 4WM on quantum memory, in particular by finding the effect of 4WM on the collective spin state.

Acknowledgments

The authors acknowledge financial support by the German Federal Ministry of Education and Research (BMBF, project QuOReP 01BQ1005).

[1] W. Tittel, M. Afzelius, T. Chaneliére, R. Cone, S. Kröll, S. Moiseev, and M. Sellars, Laser & Photonics Reviews, **4**, 244 (2010).
[2] A. E. Kozhekin, K. Mølmer, and E. Polzik, Phys. Rev. A, **62**, 033809 (2000).
[3] M. Fleischhauer, A. Imamoglu, and J. P. Marangos, Rev. Mod. Phys., **77**, 633 (2005).
[4] M. Fleischhauer and M. D. Lukin, Phys. Rev. Lett., **84**, 5094 (2000).
[5] M. Fleischhauer and M. D. Lukin, Phys. Rev. A, **65**, 022314 (2002).
[6] C. Liu, Z. Dutton, C. H. Behroozi, and L. V. Hau, Nature, **409**, 490 (2001).
[7] D. F. Phillips, A. Fleischhauer, A. Mair, R. L. Walsworth, and M. D. Lukin, Phys. Rev. Lett., **86**, 783 (2001).
[8] M. D. Eisaman, A. Andre, F. Massou, M. Fleischhauer, A. S. Zibrov, and M. D. Lukin, Nature, **438**, 837 (2005).
[9] H. Zhang, X.-M. Jin, J. Yang, H.-N. Dai, S.-J. Yang, T.-M. Zhao, J. Rui, Y. He, X. Jiang, F. Yang, G.-S. Pan, Z.-S. Yuan, Y. Deng, Z.-B. Chen, X.-H. Bao, S. Chen, B. Zhao, and J.-W. Pan, Nat Photon, **5**, 628 (2011).
[10] U. Schnorrberger, J. D. Thompson, S. Trotzky, R. Pugatch, N. Davidson, S. Kuhr, and I. Bloch, Phys. Rev. Lett., **103**, 033003 (2009).
[11] Y. O. Dudin, L. Li, and A. Kuzmich, Phys. Rev. A, **87**, 031801 (2013).
[12] J. J. Longdell, E. Fraval, M. J. Sellars, and N. B. Manson, Phys. Rev. Lett., **95**, 063601 (2005).
[13] I. Novikova, R. Walsworth, and Y. Xiao, Laser & Photonics Reviews, **6**, 333 (2012).
[14] Y.-H. Chen, M.-J. Lee, I.-C. Wang, S. Du, Y.-F. Chen, Y.-C. Chen, and I. A. Yu, Phys. Rev. Lett., **110**, 083601 (2013).
[15] A. V. Gorshkov, A. André, M. Fleischhauer, A. S. Sørensen, and M. D. Lukin, Phys. Rev. Lett., **98**, 123601 (2007).
[16] N. B. Phillips, A. V. Gorshkov, and I. Novikova, Phys. Rev. A, **78**, 023801 (2008).
[17] R. M. Camacho, P. K. Vudyasetu, and J. C. Howell, Nat Photon, **3**, 103 (2009).
[18] N. B. Phillips, A. V. Gorshkov, and I. Novikova, Phys. Rev. A, **83**, 063823 (2011).
[19] P. Kolchin, Phys. Rev. A, **75**, 033814 (2007).
[20] M. Sargent, M. Scully, and W. Lamb, *Laser Physics* (Addison-Wesley, Reading, MA, 1974).